DOI:10.31557/APJCC.2026.11.2.157

RESEARCH ARTICLE

Development of a Brachytherapy Applicator with *In-Vivo* Dosimetry Using 3d Printing Technology for the Treatment of Gynaecological Cancers

Jayapalan Krishnan[1]*, Nisma Farooq[1], Achuth S Nayak[1], D Anu[2], Bhoomika Angana[2], M Dinesh[1], Suryanarayana Kunikullaya[1], Muhammed Shafeeque[1], Bilita Parhi[1], Harikrishna Suresh[1], Divya Lakshmanan M[3], Sandhya Mohan[3]

[1]Yenepoya Medical College Hospital, Mangalore, Karnataka, India. [2]Mangalore University, Mangalore, Karnataka, India. [3]Yenepoya Research Centre, Yenepoya (Deemed to be University), Mangalore, Karnataka, India.

Abstract

Introduction: This study aimed to create a 3D-printed brachytherapy applicator with integrated in-vivo dosimetry and to find an optimal distance for the placement of peripheral catheters with a central tandem for treating gynaecological carcinoma. **Material and Methods:** A 3D-printed applicator made of polylactic acid (PLA) with detachable components for in-vivo dosimetry was created and tested on a customized water phantom using TG-43 and model based algorithm. The developed sorbo applicator was used to build a strategy for analyzing Ir-192 brachytherapy source dose distribution using a virtual water phantom. Three sets of plans were investigated, one with a central source and the others with peripheral sources, utilizing needles and flexible catheters positioned at varied radial distances from the central source. **Results:** The applicator was validated and found to have no significant changes in dosimetric and geometric features. The dose distribution with only the central source showed a rapid falloff near the source and a progressive falloff as distance increased. Peripheral sources loaded at the distance from 1.2 to 1.3 cm from the central source, resulted in improved dose asymmetry as well as reduced the dose to the organ at risk. Flexible catheters provide superior coverage. In-vivo dosimetry demonstrated optimized agreement with estimated dose. **Conclusion:** The newly developed brachytherapy applicator, made with sophisticated 3D printing technology and incorporated in-vivo dosimetry, effectively optimizes dose distribution to both the vaginal walls and the vault apex. This novel design may be a dosage-guided therapy that improves dose delivery by changing the source position and dwell time.

Keywords: Brachy applicator with In-vivo dosimetry- 3D Printed sorbo applicator- Multi-channel cylindrical applicator

Asian Pac J Cancer Care, **11 (2)**, 157-167 Submission Date: 11/26/2025 Acceptance Date: 01/04/2026

Introduction

Gynaecological malignancies, including cervical, endometrial, vaginal, vault, and ovarian tumors, have specific epidemiological and clinical characteristics [1, 2]. GLOBOCAN reported, new cancer cases that occurred due to gynaecological cancers accounted for 18% of all cancer cases and over 16% of all the deaths among women with cancer worldwide [3]. Gynaecological malignancies can be treated with surgery, chemotherapy, or radiotherapy [4, 5]. Image-guided adaptive radiotherapy has emerged as a critical strategy for treating malignant tumors. It allows customized treatment by accounting for anatomical changes during therapy [6-8].

Brachytherapy remains the most widely used treatment for gynaecological malignancies [9-11]. Applicator's design is based on patient's anatomy and disease extent and imaging modalities used for reconstruction and treatment planning in order to minimize treatment complications and improved cancer cure rates. Applicator design has advanced, incorporating three-dimensional (3D) imaging and sophisticated treatment planning,

Corresponding Author:
Dr. Jayapalan Krishnan
Yenepoya Medical College Hospital, Mangalore, Karnataka, India.
Email: nkjayapalceg37@gmail.com

making it the standard of care [12, 13].

Different applicators have unique characteristics and challenges. Single-channel cylindrical applicators (SCCA) have less planning flexibility and are only appropriate for modest tumor volumes. Some applicators limit dose escalation to crucial target volume, conserving healthy tissue [14-18]. Multi-channel cylindrical applicators (MCCA) are designed to overcome the limits of SCCA and provide enhanced planning capabilities. Commercially available applicators might be expensive and require additional settings for in vivo dosimetry (IVD).

In terms of dose distribution, ICBT typically prescribes doses to the clinical target volume (CTV) ranging from 10 cm^3 to 200 cm^3. Even in smaller CTVs, the dose distribution is heterogeneous, with lower doses near the CTV margin and significantly higher doses near the radioactive sources. As a result, the average dose and dose rate within the CTV are much higher than at the periphery. In external beam radiotherapy, dose reduction is gradual and hence larger volume of healthy tissues would get a higher dose, which would be unacceptable [19, 20]. To maximize the benefits of brachytherapy, an appropriate applicator method must be developed.

In vivo dosimetry (IVD) plays an essential role in verifying dose delivery during brachytherapy in order to confirm whether the planned dose is delivered accurately. IVD involves placing a detector near the target volume or organ at risk, often requiring invasive techniques [20, 21]. Radiochromic film based IVD, provides two-dimensional dose information and creates a permanent record of the irradiation, making them a key tool for accurate in vivo dosimetry [22, 23]. Polylactic acid (PLA) material is a biocompatible material. It has the density of 1.25 g/cm^3. It is evident from various studies that PLA is used widely to make various implant [24].

This study aimed to develop a novel 3D-printed HDR brachytherapy applicator incorporating in-vivo dosimetry, particularly for patients with unilateral disease involvement, difficult anatomy, or vaginal tumors ranging in thickness from 5 to 10mm. The primary objective was to create a biocompatible applicator that accommodated both a central tandem and peripheral catheters or needles, positioned at an optimal distances for effective treatment. The study also intended to test the applicator's physical properties to confirm its acceptability for clinical use. Plans were generated and evaluated with flexible catheters and needles at the peripheral locations relative to the central tandem. Furthermore, the study validated the accuracy of the calculated dose and compared with delivered dose at the reference point by employing EBT3 film for dosimetric verification.

Materials and Methods

Development of the applicator - material selection and biocompatible test

Polylactic acid (PLA) material was selected. Before using it to make applicator, Mouse fibroblast cell line (L-929) was used to confirm the biocompatibility of the PLA. The cells were maintained in DMEM supplemented with 10% FBS, 1% penicillin and streptomycin, and 2 mM L-glutamine, at 37oC in a humidified incubator with 5% CO_2.

Cell proliferation assay

L-929 cells were plated at a density of $0.1x10^6$ cells/ml per well in a 6-well plate (Falcon, Corning, India) and incubated for 24 hours. Base material and PLA were added to respective plate. After incubation for 24 hours, cells were trypsinised and 100 ul of the cell suspension was added to a 96 well plate and MTT assay was performed immediately as mentioned previously (Shaheer et al., 2020). The color developed was quantified using a microplate reader at 570 nm. Cell proliferation was calculated using the equation,

Percentage of cell proliferation = (Absorbance of cells in control- Absorbance of cells in test)*100/ The absorbance of cells in control

Colony forming assay

Cells were seeded at a density of 100 cells/well in a 6-well plate (Falcon, Corning, India) and incubated for 14 days. Base material and PLA were added after 24 h of cell seeding, to the respective plate. Media was changed every 3 days. After treatment for 14 days, colony formation was assed.

3D printing, verification of the applicator's position and radiological properties

WOL3D Creality Ender 3 Pro Model (Creality, Shenzhen Creality 3D Technology Co., Ltd., Guangdong, China) 3D printer was used. Using this printer, the volume up to 220x220x250 mm3 can be printed. FDM (Fused Deposition Modelling) technology was used to make a polylactic acid (PLA) applicator [25, 26]. CATIA (Computer Aided Three-Dimensional Interactive Application) software was used to make the design the work. It uses nozzle temperature from 190° C to 230° C to print the PLA material and the applicator was printed with 100 % infill.

Steam heated sterilization involves temperatures ranging from 121 to 134°C under pressure. The higher temperatures used in the process could affect the structure of the PLA applicator [27]. Therefore, ETO sterilization procedures are recommended for the applicator disinfection.

It had a diameter of 30mm, a length of 140mm, and a 300 degree curvature at the tip. It consists of five detachable parts: the external body, the internal body, components for installing TLD and films, compensatory materials for beam modulation, and a fixation cap with stopper buttons.

The internal body is developed to accommodate eight peripheral catheters at an appropriate distance of 12mm from the central source, spaced 45° apart, with 300 curvatures at the tip. Two sets of four detachable components for in vivo dosimetry (IVD) were created, one for TLD capsules spaced 10mm apart and another for inserting Gafchromic film in the source axial direction

with a length of 125mm. In the absence of in vivo dosimetry, these detachable components can be filled with a compensatory substance. Once all four components have been inserted and the cap has been affixed to hold them in place. Both the side of the fixation cap, fixation buttons were placed to fix the catheter. The catheter position and reproducibility tests were done by autoradiograph method. The central tandem can go through the cavity produced at the center (Figures 1 and 2).

To verify the physical and radiological properties, a simple water phantom was created as shown in the Figure 3. The developed applicator was inserted in the phantom, with two slots carrying EBT3 Gafchromic films on its apex end. Two setups were used. In first setup, a titanium intrauterine probe in the center cavity and eight needles at the periphery; in the second setup, the needles were replaced with flexible catheters. CT images of both setups were acquired with the slice thickness of 1.25mm using a Wipro GE IQ gen 2 PET-CT. Physical parameters such as the dimension of the applicator, angle between successive peripheral catheters, and the angle of curvature at the tip of the applicator were checked. Radiological properties such as Hounsfield (HU) number and the material heterogeneity were verified using CT image tools and a model based 3D dose calculation algorithm BVAcuros (16.1 version) by comparing with TG-43 based dose calculation.

Ir-192 brachytherapy source dose distribution at different loading pattern

To better understand the dose distribution from the Ir-192 source, a plan was generated using Eclipse Treatment Planning System (TPS) 16.1 and a 30mm diameter vaginal cylindrical applicator. The dose fall

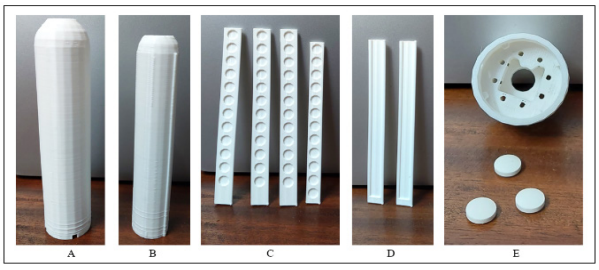

Figure 1. The Parts of a 3D Printed Brachytherapy Applicator. A) External body; B) Internal body; C) Components for TLD placement D) Components for film placement; and E) Fixation cap and 3D-printed compensating buttons

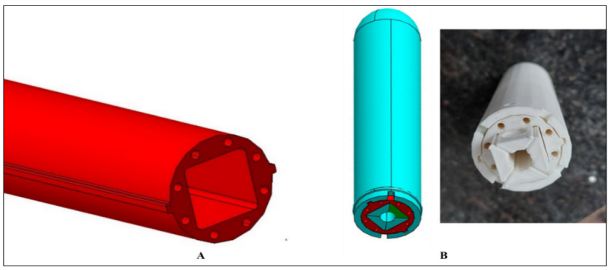

Figure 2. A) Internal Body with Peripheral Source Transfer Channels B) Assembled Applicator

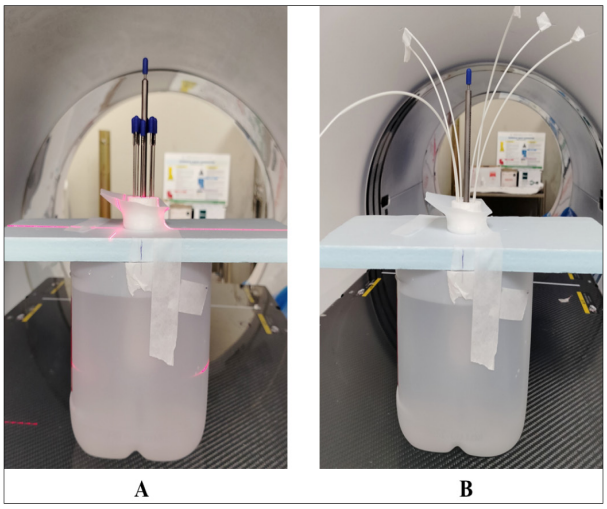

Figure 3. Phantom with Applicator, Central Tandem and Needles at the Peripheral Channels (A) and Flexible Catheters at the Peripheral Channels (B).

off was analyzed across and along the source axis using a single central source located at the tip of the cylinder and normalized at 1cm from the applicator's surface, as shown in Figure 4.

To visualize the dose distribution of the loaded source, a point along the central source was selected as the dwell position, with a reference point set at 5 mm from the applicator's surface in the same plane. The dose was initially normalized to 1 Gy at the point, followed by another identical plan was created with the prescription of 10 Gy to the same point. For both recommended dosages, the dose fall-off was measured in terms of the distance at each 10% dose reduction from the normalized point.

Three sets of plans were created, one with a central source alone and the other two with peripheral sources loaded symmetrically in all directions utilizing needles and flexible catheters, as illustrated in Figures 5a, 5b, and 5c respectively. To create an asymmetric dose distribution, doses were normalized at either the unilateral target volume or the ipsilateral reference point. Meanwhile, the surface dose on the contralateral side was kept as close as possible to the specified amount. To determine the best catheter placement in the radial direction from the central source, peripheral sources were loaded at different distances of 1.5 cm, 1.3 cm, 1.2 cm, and 1.0 cm from the central source. The optimum distance between central tandem and peripheral needles/catheters was calculated. To further understand the role of the central source when using peripheral sources, a plan with solely peripheral sources and a 1 Gy dose normalized to the same reference point was investigated.

Preclinical validation

Brachytherapy plans were created and catheter reconstruction was carried out on both the CT images using Eclipse TPS. One uses a needle, while the other uses flexible catheters with 1.25mm steps. A reference line was drawn at 5mm from the surface of the applicator. The 192Ir source was loaded at 3mm steps from the apex of the applicators and catheters and extended up

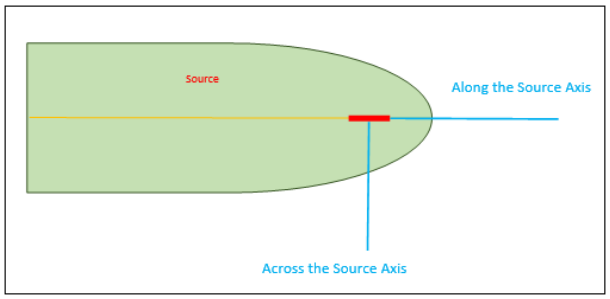

Figure 4. Schematic Diagram of Vaginal Cylindrical Applicator and Source Dwell Position

to 5cm. Dwell time was calculated for 1Gy dose at the reference line, both with and without peripheral needles and catheters. The dose was calculated using both the manual and volumetric optimization methods. The dose distribution was analyzed. A Gafchromic film strip was inserted at the given provision for IVD. The analysed volumetric optimized plan was executed using the Varian GammaMed iX Plus HDR brachytherapy unit on the customised phantom with the simillar setup. The exposed film was scanned using Epson 11000XL scanner and SNC Patient (Sun Nuclear Corporation) film dose analyser that was calibrated upto 15Gy using Ir-192 source. The measured dose at the various points along the reference line was determined compared with TPS calculated dose. For the purpose of the reproduciability, point dose measutement was repeated for five trails.

Besides, an asymmetric GTVp volume was drawn on the CT images, and plans were created and dose was prescribed to the target volume GTVp. Source was loaded at the peripheral catheters and the dose was normalised to the target volume. Simillarly, one more plan with needles at the peripheral was done. Tumor coverage for both plans was compared to determine the relevance of the curve at the applicator's apex, which only allows the flexible catheter to pass. Finally, a plan with only the central tandem was created to simulate the routine practice conditions. Using Dose Volume Histogram

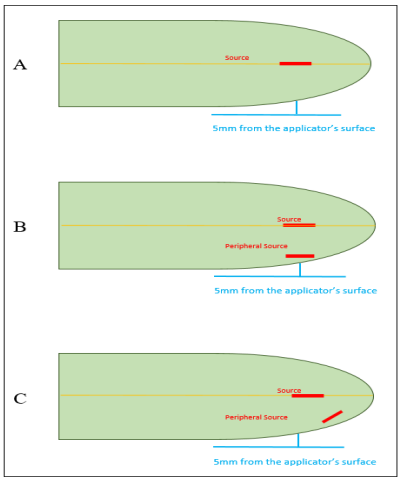

Figure 5. A Schematic Representation of the Vaginal Cylindrical Applicator's source Loading Pattern. A-Central Source alone; B-Central Source and peripheral source loaded with needle; C-Central Source and peripheral source loaded with flexible catheter.

(DVH), D98%, D90%, D50%, and V150% values for the GTVp were recorded and compared between the plans as per ICRU89.

Results

Development of the applicator - material selection and biocompatible test

Figure 6 shows that the PLA is biocompatible to the cells. The MTT assay showed that PLA is compatabile with the cells. Both PLA and the Base-treated group showed no significant (ns) change in relative proliferation compared to the untreated control, confirming its compatibility. Consistent with these findings, the colony forming assay demonstrated that PLA treatment promoted long-term cell survival, as evidenced by an increased number of visible colonies (**$p < 0.001$) and the results were comparable to that of the untreated control. Base material treatment, on the other hand, resulted in a moderate reduction in colony formation compared to the untreated control (**$p < 0.001$); however, cells remained viable and capable of forming colonies. Collectively, these results indicate that PLA is biocompatible and supports both proliferation and long-term survival, highlighting its potential suitability for biomedical applications.

3D printing, verification of the applicator's position and radiological properties

The measured outer diameter and the length of the applicator was 30mm and 140mm respectively. The result ensured that the differences in the dimension was <1.0 mm between the modelled and printed applicator. The applicator's average HU value at multiple spots was +131.87±2.48. It shows that the material is PMMA-equivalent one. The measured angle between the successive peripheral catheters was 44.60 ± 0.60. At the tip of the applicator, the measured converged angle of the projected flexible catheters from its axis was 30.20. The auto radiograph shows the catheter position and reproducibility was achieved within 1mm.

Figure 7 shows TPS calculated dose across the sorbo applicator with needle using TG-43 (blue) and BVAcuros (red). The calculated dose in the sorbo applicator using both TG-43 and BVAcuros algorithm shows good aggrement except at the central tandem and needles

Table 1. The Surface Dose at the Ipsilateral and Contralateral Side Using Central Tandem and the Peripheral Source at Various Distances from the Applicator's surface after Normalized to the Reference Point at 5mm from the Surface of the Applicator

Distance from the centre tandem and unilateral peripheral catheter (mm)	Applicator's Surface dose (%)	
	ipsilateral (treatment side)	Contralateral side
15	318	80
13	155	112
12	142	120
10	125	134

location where dose spikes were resulted. It is due to unaccounting the material properties in the calcualtion using TG-43.

Ir-192 brachytherapy source dose distribution at different loading pattern

Figure 8 illustrates the dose distribution for the design with a single central source inside the virtual applicator. The inverse square law resulted in a quick dose fall off near the source, which became more gradual as distance increased. Furthermore, the spacing between successive isodose lines was independent of the prescribed dose.

The dose rate fall-off remained consistent whether the dose was 1Gy or 10Gy. Furthermore, the distance between the 100% and 90% isodose lines is only about 1 mm, whereas the distance between the 20% and 10% isodose lines is substantially longer, roughly 18 mm. This demonstrates that the rate of fall-off at higher dose levels is sharper than at lower dose levels, which is gradual.

Because of the source's self-attenuation, an anisotropic dose distribution was observed, as shown in Figure 8, resulting in varying levels of exponential decay with respect to dose at the source's outer layer along different axes. Figure 9 depicts the observed dose fall-off along and across the source axis from the source's outer layer.

As distance increases, the disparities in dose rate fall-off decrease, and normalization with regard to a point on either axis may become more similar. Using this graph, the reference point dose at the center plane of the source axis was calculated using equations 1 and 2.

$$D^{C}_{Ref\ point} = 5710 \text{ X } e^{-2.873x} - x^2 \quad \text{---------- (1)}$$

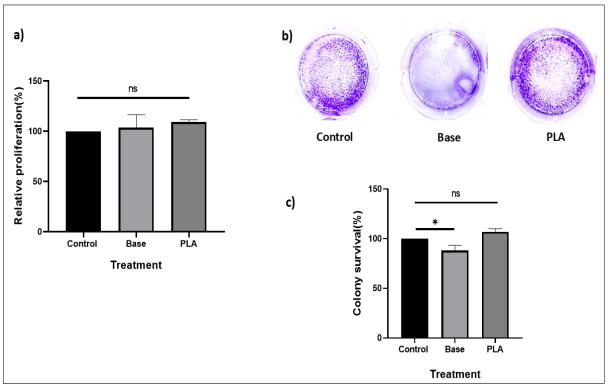

Figure 6. PLA is Biocompatible to the Cells. a) MTT assay showing relative cell proliferation (%) of L929 cells at 24 h of incubation. Data are represented as mean ± SD (n =3). (b) Representative images from the Clonogenic assay. (c) Quantification of colony formation expressed as relative colony number.

Dose summation of central and peripheral catheters contribution is

$$D^{C\ and\ P}_{Ref\ point} = \sum_{i=1}^{i=n} [\, W_{i=0}^{i=1} \ 5710 \text{ X } e^{-2.873x} - x^2 \,] \quad \text{---------- (2)}$$

Where C is central tandem, P is peripheral catheters combination, W is dose contribution weightage from central and peripheral source.

Even though a dose of 1 Gy was provided on either side of the applicator, the dose distribution remained symmetrical on both sides (Figure 10 A). This can result in an unintentional increased dose to healthy tissues, similar to the treatment side. However, by adding a peripheral source to the central one, the dose symmetry was altered. This reduces the excess dose provided to healthy tissue

Table 2. TPS Calculated vs. Measured dose Using Film IVD at Different Positions

Different points at 1cm from the central tandem along the source axial line (cm)	Dose calculated in TPS TPS calculated dose (cGy)	Dose measured from Film dosimetry (cGy)
0	97	99.69
0.5	89	87.1
1	87.3	88.6
1.5	86.6	81.8
2	97	99.69
2.5	64	62

Table 3. Dose Statistics of GTV_p Target. The plan with flexible tube and central tandem shows better target dose coverage and reduced the hotspot volume than other plans.

Dose volume parameters (GTV_p)	Relative dose and volume of various plans (%)			
	Flexible catheter with Central tandem	Needle with Central tandem	Flexible catheter without Central tandem	Needle without Central tandem
$D_{98\%}$	87	75	105.9	82
$D_{90\%}$	100.1	88.4	118	98
$D_{50\%}$	120	131	163	176
$V_{150\%}$	29.3	29.3	61.7	62.8
$V_{200\%}$	4.9	9.8	24.5	39.1

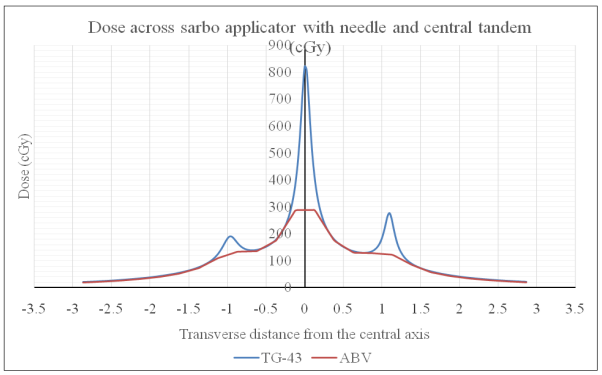

Figure 7. TPS Calculated Dose Across the Sorbo Applicator with Needle Using TG-43 (blue) and BVAcuros (red).

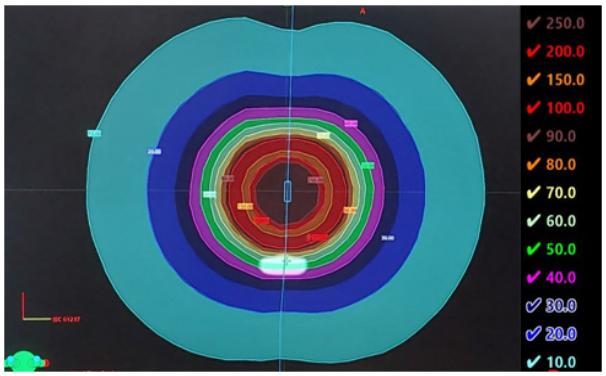

Figure 8. Dose Distribution Obtained by Placing Only a Central Source

on the untreated side (Figure 10 B). The weightage of the dwell time for each source effects the asymmetric dose distribution, which varies based on clinical demands.

With only the central source, normalized to a point 5 mm from the applicator's surface, a steep dose gradient occurred within the applicator, resulting in an applicator surface dose of 170%. However, when the peripheral source was included, the isodose distribution shifted.

Table 1 shows that the surface dose at the ipsilateral and contralateral side using central tandem and the peripheral source at various distances from the applicator's surface after normalized to the reference point at 5mm from the surface of the applicator.

The peripheral source is loaded on the applicator's surface with 10% of the central source contribution; the tumor side surface receives almost 300% of the prescribed dose, risking damage to the vaginal mucosa, while the opposite side is under-dosed by 20% of the prescribed dose. Moving the peripheral source inward reduces the hotspot volume while increasing the dose on the contralateral (under-dosed) side, resulting in better dose distribution. However, moving the peripheral source too near to the central source causes the dose distribution to become symmetric. By shifting the peripheral source by 1mm increments, the ideal distance to ensure satisfactory dose coverage without increasing the hotspot volume was discovered to be between 1.2 cm and 1.3 cm.

Furthermore, loading the source only in the peripheral catheters with no contribution from the central source resulted in 430% of the specified dose reaching the vaginal mucosa, which was excessive and undesirable. Despite moving the normalization point closer to the surface to minimize the surface dose, the mucosa dose remains higher while the target coverage is reduced.

Preclinical validation

Figure 11 displays the reconstruction of needles and catheters from obtained CT images. Flexible catheters could pass through the curvature at the applicator's apex, but needles were halted where it began.

Figure 12 (A) illustrates the dose distribution using the center tandem alone. The dose normalization with the central source failed to account for the target's uneven thickness.

Figure 12 (B) and 12 (C) shows manually optimized dose distribution with peripheral sources loaded with needles and loaded with flexible catheters along with central source for the given target volume GTVp respectively. Peripherally loaded sources in combination with central tandem provided better dosage coverage than central tandem alone. Similar results were obtained using the volumetric optimized plan, as shown in Figure 13. At the apex, the volumetric optimized flexible catheters plan (Figure 14 (B)) enhanced lateral dose distribution marginally while decreasing hot volume compared to the manually optimized plan (Figure 14 (A)). Figure 15 shows Dose volume histogram of GTVp target. The plan with flexible tube and central tandem shows better target dose coverage and reduced the hotspot volume than other plans

The IVD results showed higher agreement with the

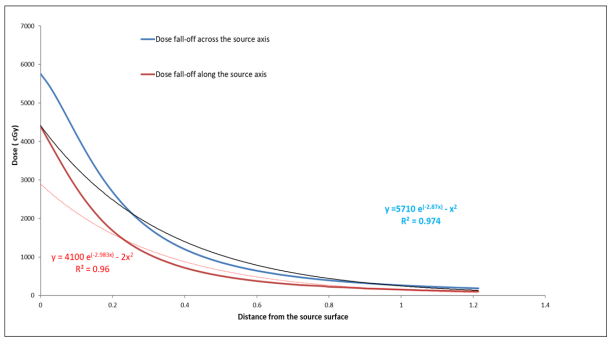

Figure 9. The Dose Distribution Across and Along the Source Orientation

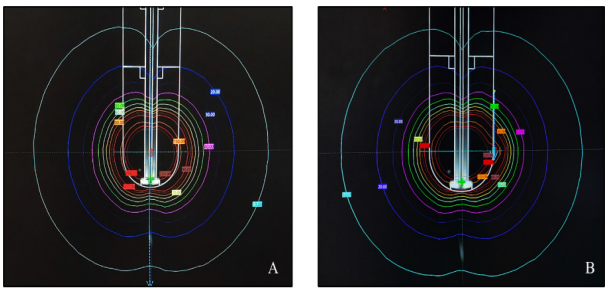

Figure 10. The Coronal View of Isodose Distribution Obtained for Dose Prescription of 1Gy to the Reference Point at the Either Side of the Applicator. A) With only a central source B) with a central source and a peripheral source near the surface of the applicator.

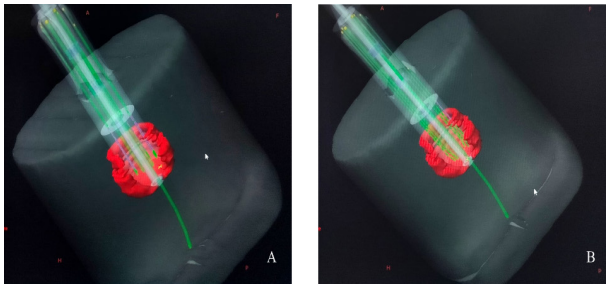

Figure 11. Reconstructed Images Showing A) Needles and B) Catheters. The red volume represents the GTV_p

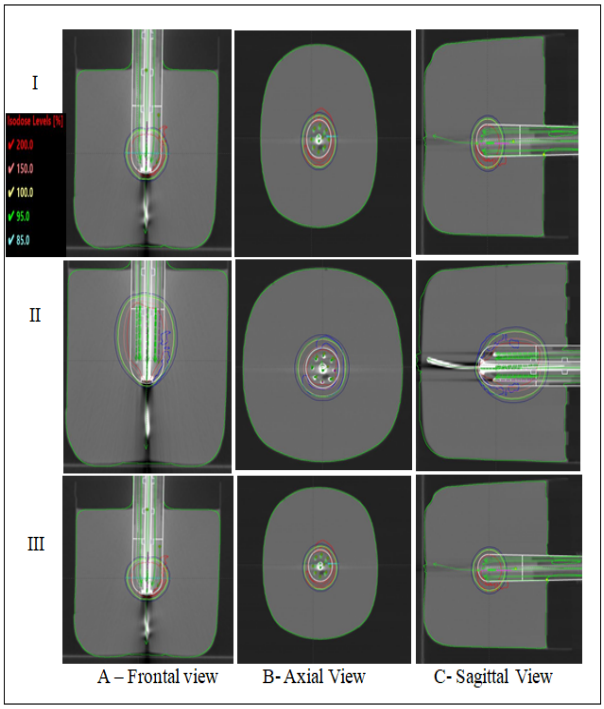

Figure 12. Dose Distribution Obtained with Central Tandem Alone (I), Manually Optimized Dose Distribution with Peripheral Sources Loaded with Needles (II) and Loaded with Flexible Catheters (III) along with Central Source for the Given Target Volume GTV_p

TPS estimated dose, and the data are shown in Table 2. Figures 16 A and B represent the TPS dose-irradiated film with ruler, respectively.

Table 3 shows the dosimeric data, such as D98%, D90%, D50% and V150% values for GTVp, were compared for various combination schemes using flexible catheters and needles, with and without the central tandem (Figure 17). A source loaded with peripheral catheters/ needles in conjunction with a central tandem provided a better dosimetric result.

Discussion

The biocompatibility assessment is mandatory process and one of the first experiments conducted for any materials developed for biomedical applications [28]. Our results indicate that PLA exhibits high compatibility with L-929 fibroblast cells, a standard cell line used for cell cytotoxicity assays. The MTT assay, which measures mitochondrial succinate dehydrogenase activity, as an indirect measure for cell viability and proliferation showed that both PLA and the Base material did not induce any significant cytotoxicity up to 24 hours of PLA exposure. The relative cell proliferation remains more or less unaltered indicating that the tested materials doesn't interfere with the short-term metabolic activity of the cells [29]. This initial compatibility is a promising measure, suggesting that the materials are not acutely toxic and do not leach harmful substances that could compromise cell health in the short term.

While the MTT assay indicates immediate biocompatibility, the clonogenic assay specifies long-term cell survival. PLA treatment not only maintained but significantly promoted the formation of colonies compared to the untreated control. This is a strong indication that PLA provides a favourable environment that supports not just cell survival, but active proliferation for a long-term. This is in accordance with other studies using PLA materials showing its biocompatibility [30]. This property is an important criterion for materials developed for applications like tissue engineering scaffolds or implantable devices, where compatibility with host tissue environment and long-term stability are mandate [31].

In this study, we used 3D printing technology to create an MCCA. Various 3D printing technologies, such as fused deposition modelling (FDM), selective laser sintering, stereo lithography, binder jetting, multi jet fusion, and micro stereo lithography, can achieve precision of less than 10µm. Biocompatibility, serializable and homogeneous printing products, and the necessity to account water equivalency (especially for TPS with TG-43 algorithm) for brachytherapy have limited the sorts of materials that may presently be printed using 3D techniques [26]. Our investigation utilized PLA with a density of 1.25 g/cm³. PLA has a HU range of +131.87±2.48, making it more water-equivalent than normal acrylic applicators with a HU of +287 [25]. Due to systematic error with 1mm deviation in the source position, the target coverage changes 2% [21, 32]. In this study, the autoradiograph ensures the catheter position and reproducibility between

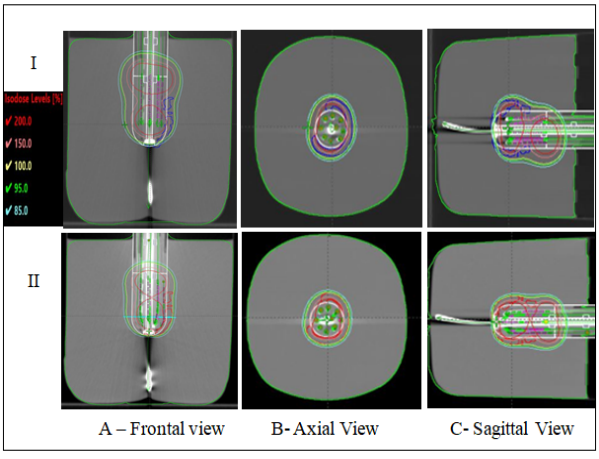

Figure 13. Volumetrically Optimized Dose Distribution Using Peripheral Sources Loaded with Needles (I) and Flexible Catheters (II), Coupled with the Central Source for the Given Target Volume GTV_p

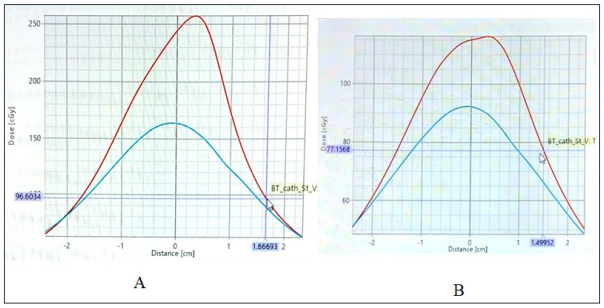

Figure 14. Dose Profile Across the Source Axis at the Applicator Tip. Manual optimization (A) and Volume optimization (B) plans with peripheral sources loaded with needles (blue line) and flexible catheters (red line), combined with the central source.

planned and delivered was within 1mm. Superimposing the pre calculated dose using a homogeneous water phantom on a clinical target volume does not consider the impact of tissue and material heterogeneity. This may lead to either under or over dose. Accounting the medium heterogeneity or using water equivalent material may help to minimize the calculation uncertainties [33]. The dose agreement between the model based algorithm and TG-43 ensures that the used PLA material for developing a 3D applicator does not affect the dose calculation. Therefore, 3D printed PLA applicator can be used for routine clinical use.

Brachytherapy is used in treatment to escalate tumor dosage, resulting in effective tumor control with minimal treatment-related toxicity. The most commonly utilized isotopes are 192Ir and 60Co. The dose fall-off near the source is substantial, with each 1mm increase in distance resulted in a further 10% dose decrease. This dose fall rate gradually decreases as distance increases. Using this information, it is possible to decide where to place the source in or near the tumour using treatment-specific applicators. The design and geometry of the applicator are crucial since dose deposition is mostly determined by distance parameters. To achieve the treatment goal, the applicator must be carefully chosen based on the anatomy and location of the tumour.

A few research emphasized the benefits of various applicators. These investigations found that the majority of vaginal cuff brachytherapy in endometrial cancer treatments was performed using an SCCA rather than colpostats or vaginal moulds because to convenience of placement, wider availability, and simpler planning [10, 34]. However, MCCA provides for greater conformal dosimetry and decreases doses to the bladder and rectum. [14]. Kim et al. [17] studied about multi-channel and single-channel cylinder applicators for the treatment of vaginal cancer. As previously stated, the SCCA is limited in its ability to achieve flexibility for dosage adjustment and conform to a variety of CTV geometry. The MCCA provides a balanced approach by combining greater dose conformity similar to interstitial approaches while also ensuring that treatment can be administered as an outpatient. The MCCA produced better dosimetry results for a lesion that was approximately 7 mm deep. However, the author proposed that interstitial brachytherapy be employed when the depth of the lesion is greater than 10mm in order to lower vaginal surface exposure while still giving the prescribed dose for thicker tumors.

Many applicators have been developed in recent years, including the multichannel Miami applicator, which can lower the dose to vital tissues while increasing the mean dose to the vaginal wall when the tumor is placed on the vaginal cuff. However, the applicator's cost is rather high [35].

Several studies have shown that advancements in 3D printing technology has been utilized to make patient specific 3D printed applicator [36-38]. A study reported that a patient-specific cylindrical vaginal applicator with oblique guide holes, developed through 3D modelling and printing techniques, allows for customized multi-channel applicators with oblique needles, tailored to the size and location of the tumour, offering improved tumor coverage [39].

Our findings show that a single central source, coverage falls short in the lateral direction; thus, peripheral sources

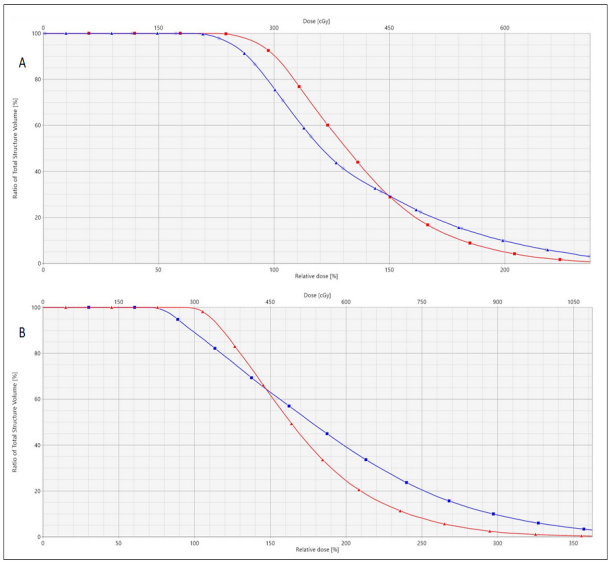

Figure 15. Dose Volume Histogram of GTVp Target. Manual optimization (A) and Volume optimization (B) plans with peripheral sources loaded with needles (blue line) and flexible catheters (red line), combined with the central source.

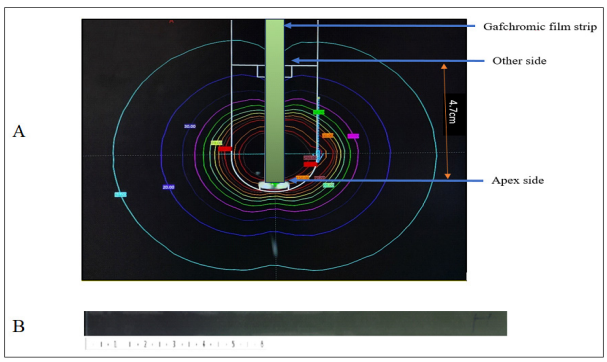

Figure 16. A) A Schematic Diagram Showing the Gafchomic Film Inside the Applicator and the Distance from the Applicator's apex where the Film Readings were Started up to 2.5cm in the Axial Line. B) Irradiated films with ruler

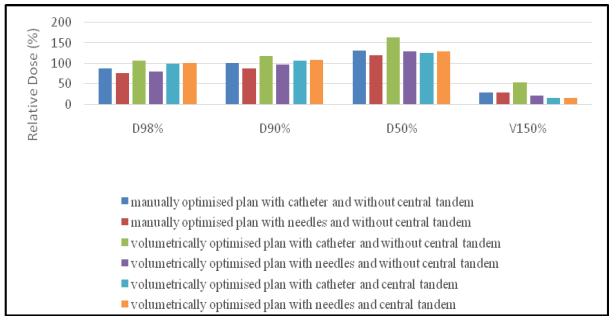

Figure 17. Shows $D_{98\%}$, $D_{90\%}$, $D_{50\%}$ and $V_{150\%}$ Values for GTV_p for the Plans with Catheters and Needles, with and without Considering the Central Tandem

are essential for resolving this constraint, especially when asymmetrical dosage distribution is necessary. This study also highlighted the benefits of flexible catheters in providing maximum coverage at the apex and lateral direction through volumetric optimization. Therefore, an in-house developed 3D applicator with many channels for source loading and dose optimization to provide superior dosimetry results with affordable cost than commercially available applicators may help to achieve better plan. Since the usage of many catheters and dwell time optimization, the positional accuracy and channel specification are vital. To confirm the delivery accuracy or alter the dose of the subsequent fraction, an in-vivo dosimetry system is needed. By providing an inherent IVD options, dose guided therapy is possible. Majority of the multichannel applicators do not have the provision for IVD [25, 36]. In our study, IVD provisions were made for both film and TLD. It can be used as both a verification tool and a dose guide for the subsequent fraction by taking into account the variance in the observed dose at a specific location in the designed applicator with the diameter of 30mm; however it is possible to print any diameter and length for each patient [40]. The feasibility of the in-vivo dosimetry can help to deliver the prescribed dose confidently. Film base IVD is a time consuming and the uncertainties while using it for the clinical purpose are to be studied.

In order to continue this research, a pilot trial would be done in patients to statistically assess target coverage and organ at risk doses using a 3D-printed MCCA and SCCA method. Patients treated with this applicator would achieve the correct dose distribution while minimizing the dose to OARs. Further applicator development would be carried out to cover large tumors that reach to the lateral parametrium.

In conclusion, the newly developed bio-compatible brachytherapy applicator, fabricated using advanced 3D printing technology and integrated in-vivo dosimetry, successfully optimizes dosage distribution to both the vaginal walls and the cuff. This novel design improves dosage delivery by adjusting the source position and dwell time. The applicator may improve clinical outcomes by improving dosage uniformity and coverage in crucial locations. Overall, this breakthrough represents a huge step forward in the field of brachytherapy, offering more effective and safer treatment alternatives for patients.

Funding

No funding has been raised for this article's work by any of the authors.

Competing interest

The authors have no financial or proprietary interests in any material discussed in this article.

Ethical Approval

Not Applicable since it's a phantom based study.

Informed consent

Not Applicable since no human or specimens participated.

Originality Declaration for Figures

All figures included in this manuscript are original and have been created by the authors specifically for the purposes of this study. No previously published or copyrighted images have been used. The authors confirm that all graphical elements, illustrations, and visual materials were generated from the data obtained in the course of this research or designed uniquely for this manuscript.

References

1. Kataki AC, Tiwari P, Thilagavthi R, Krishnatreya M. Epidemiology of gynaecological cancers. Fundamentals in gynaecologic malignancy. Springer. 2023;:1-8.
2. Schüler-Toprak S, Seitz S, Ortmann O. Hormone und das risiko für brustkrebs und gynäkologische malignome: Ein systematisches review. Der Gynäkologe. 2017;50:43-54.
3. Zhu B, Gu H, Mao Z, Beeraka N, Zhao X, Anand M. Global burden of gynaecological cancers in 2022 and projections to 2050. J Glob Health. 2024;14(04155). https://doi.org/10.7189/jogh.14.04155.
4. Javadinia S, Masoudian M, Homaei Shandiz F. Local control and overall survival of patients with stage iib–iva cervical cancer after definitive external beam chemoradiation and high-dose-rate cobalt-60 intracavitary brachytherapy. Indian Journal of Gynecologic Oncology. 2020;18(1). https://doi.org/10.1007/s40944-019-0364-4.
5. Homaei Shandiz F, Arastouei S, Hosseini S, Prasad Giri I, Javadinia SA, Dayanni M. Capecitabine-enhanced brachytherapy in locally advanced cervical cancer: A phase ii non-randomized trial on safety and efficacy. Cancer Invest. 2025;43(4):244–56. https://doi.org/10.1080/07357907.2025.2493238.
6. Viswanathan A, Thomadsen B, American Brachytherapy Society Cervical Cancer Recommendations C, American Brachytherapy S. American brachytherapy society consensus guidelines for locally advanced carcinoma of the cervix. Part i: General principles. Brachytherapy. 2012;11(1):33–46. https://doi.org/10.1016/j.brachy.2011.07.003.
7. Banerjee R, Kamrava M. Brachytherapy in the treatment of cervical cancer: A review. Int J Womens Health. 2014;6:555–64. https://doi.org/10.2147/IJWH.S46247.
8. Park H, Suh C, Kim G. Fractionated high-dose-rate brachytherapy in the management of uterine cervical cancer. Yonsei Med J. 2002;43(6):737–48. https://doi.org/10.3349/ymj.2002.43.6.737.

9. Nag S, Erickson B, Parikh S, Gupta N, Varia M, Glasgow G. The american brachytherapy society recommendations for high-dose-rate brachytherapy for carcinoma of the endometrium. Int J Radiat Oncol Biol Phys. 2000;48(3):779–90. https://doi.org/10.1016/s0360-3016(00)00689-1.
10. Sabater S, Andres I, Lopez-Honrubia V, Berenguer R, Sevillano M, Jimenez-Jimenez E. Vaginal cuff brachytherapy in endometrial cancer - a technically easy treatment?. Cancer Manag Res. 2017;9:351–62. https://doi.org/10.2147/CMAR.S119125.
11. Karlsson J, Dreifaldt A, Mordhorst LB, Sorbe B. Differences in outcome for cervical cancer patients treated with or without brachytherapy. Brachytherapy. 2017;16(1):133-140. https://doi.org/10.1016/j.brachy.2016.09.011
12. Mourya A, Aggarwal LM, Choudhary S. Evolution of Brachytherapy Applicators for the Treatment of Cervical Cancer. Journal of Medical Physics. 2021;46(4):231-243. https://doi.org/10.4103/jmp.jmp_62_21
13. Dimopoulos JCA, Petrow P, Tanderup K, Petric P, Berger D, Kirisits C, Pedersen EM, et al. Recommendations from Gynaecological (GYN) GEC-ESTRO Working Group (IV): Basic principles and parameters for MR imaging within the frame of image based adaptive cervix cancer brachytherapy. Radiotherapy and Oncology: Journal of the European Society for Therapeutic Radiology and Oncology. 2012 04;103(1):113-122. https://doi.org/10.1016/j.radonc.2011.12.024
14. Demanes D, Rege S, Rodriquez RR, Schutz KL, Altieri GA, Wong T. The use and advantages of a multichannel vaginal cylinder in high-dose-rate brachytherapy. International Journal of Radiation Oncology*Biology*Physics. 1999 04;44(1):211-219. https://doi.org/10.1016/S0360-3016(98)00453-2
15. Tanderup K, Lindegaard JC. Multi-channel intracavitary vaginal brachytherapy using three-dimensional optimization of source geometry. Radiotherapy and Oncology. 2004 01;70(1):81-85. https://doi.org/10.1016/j.radonc.2003.11.006
16. Kim H, Kim H, Houser C, Beriwal S. Is there any advantage to three-dimensional planning for vaginal cuff brachytherapy?. Brachytherapy. 2012;11(5):398-401. https://doi.org/10.1016/j.brachy.2011.12.009
17. Kim H, Rajagopalan MS, Houser C, Beriwal S. Dosimetric comparison of multichannel with one single-channel vaginal cylinder for vaginal cancer treatments with high-dose-rate brachytherapy. Brachytherapy. 2014 05;13(3):263-267. https://doi.org/10.1016/j.brachy.2013.08.009
18. Beriwal S, Bhatnagar A, Heron DE, Selvaraj R, Mogus R, Kim H, Gerszten K, Kelley J, Edwards RP. High-dose-rate interstitial brachytherapy for gynecologic malignancies. Brachytherapy. 2006 Oct;5(4):218-222. https://doi.org/10.1016/j.brachy.2006.09.002
19. De Brabandere M, Mousa AG, Nulens A, Swinnen A, Van Limbergen E. Potential of dose optimisation in MRI-based PDR brachytherapy of cervix carcinoma. Radiotherapy and Oncology. 2008 08;88(2):217-226. https://doi.org/10.1016/j.radonc.2007.10.026
20. Mijnheer B, Beddar S, Izewska J, Reft C. In vivo dosimetry in external beam radiotherapy. Medical Physics. 2013 07;40(7):070903. https://doi.org/10.1118/1.4811216
21. Fonseca GP, Johansen JG, Smith RL, Beaulieu L, Beddar S, Kertzscher G, Verhaegen F, Tanderup K. In vivo dosimetry in brachytherapy: Requirements and future directions for research, development, and clinical practice. Physics and Imaging in Radiation Oncology. 2020 Oct;16:1-11. https://doi.org/10.1016/j.phro.2020.09.002
22. Tanderup K, Beddar S, Andersen CE, Kertzscher G, Cygler JE. In vivo dosimetry in brachytherapy. Medical Physics. 2013 07;40(7):070902. https://doi.org/10.1118/1.4810943
23. Moylan R, Aland T, Kairn T. Dosimetric accuracy of Gafchromic EBT2 and EBT3 film for in vivo dosimetry. Australasian Physical & Engineering Sciences in Medicine. 2013 09;36(3):331-337. https://doi.org/10.1007/s13246-013-0206-0
24. Shilov SY, Rozhkova YA, Markova LN, Tashkinov MA, Vindokurov IV, Silberschmidt VV. Biocompatibility of 3D-Printed PLA, PEEK and PETG: Adhesion of Bone Marrow and Peritoneal Lavage Cells. Polymers. 2022 09 22;14(19):3958. https://doi.org/10.3390/polym14193958
25. Van der Walt M, Crabtree T, Albantow C. PLA as a suitable 3D printing thermoplastic for use in external beam radiotherapy. Australasian Physical & Engineering Sciences in Medicine. 2019 Dec;42(4):1165-1176. https://doi.org/10.1007/s13246-019-00818-6
26. Ricotti R, Vavassori A, Bazani A, Ciardo D, Pansini F, Spoto R, Sammarco V, et al. 3D-printed applicators for high dose rate brachytherapy: Dosimetric assessment at different infill percentage. Physica medica: PM: an international journal devoted to the applications of physics to medicine and biology: official journal of the Italian Association of Biomedical Physics (AIFB). 2016 Dec;32(12):1698-1706. https://doi.org/10.1016/j.ejmp.2016.08.016
27. Pérez Davila S, González Rodríguez L, Chiussi S, Serra J, González P. How to Sterilize Polylactic Acid Based Medical Devices?. Polymers. 2021 06 28;13(13):2115. https://doi.org/10.3390/polym13132115
28. Rosa V, Silikas N, Yu B, Dubey N, Sriram G, Zinelis S, Lima AF, et al. Guidance on the assessment of biocompatibility of biomaterials: Fundamentals and testing considerations. Dental Materials. 2024 Nov;40(11):1773-1785. https://doi.org/10.1016/j.dental.2024.07.020
29. Kumar P, Nagarajan A, Uchil PD. Analysis of Cell Viability by the MTT Assay. Cold Spring Harbor Protocols. 2018 06;2018(6):pdb.prot095505. https://doi.org/10.1101/pdb.prot095505
30. Ahuja R, Kumari N, Srivastava A, Bhati P, Vashisth P, Yadav P, Jacob T, Narang R, Bhatnagar N. Biocompatibility analysis of PLA based candidate materials for cardiovascular stents in a rat subcutaneous implant model. Acta Histochemica. 2020 Oct;122(7):151615. https://doi.org/10.1016/j.acthis.2020.151615
31. Krajovic DM, Kumler MS, Hillmyer MA. PLA Block Polymers: Versatile Materials for a Sustainable Future. Biomacromolecules. 2025 05 12;26(5):2761-2783. https://doi.org/10.1021/acs.biomac.5c00161
32. Tanderup K, Hellebust TP, Lang S, Granfeldt J, Pötter R, Lindegaard JC, Kirisits C. Consequences of random and systematic reconstruction uncertainties in 3D image based brachytherapy in cervical cancer. Radiotherapy and Oncology. 2008 Nov;89(2):156-163. https://doi.org/10.1016/j.radonc.2008.06.010
33. Srivastava S, Kannathuparambil Venugopal A, Nara Singh M. Effect of model-based dose-calculation algorithms in high dose rate brachytherapy of cervical carcinoma. Reports of Practical Oncology and Radiotherapy. 2024 07 22;29(3):300-308. https://doi.org/10.5603/rpor.100778
34. Harkenrider MM, Grover S, Erickson BA, Viswanathan AN, Small C, Kliethermes S, Small W. Vaginal brachytherapy for postoperative endometrial cancer: 2014 Survey of the American Brachytherapy Society. Brachytherapy. 2016 01;15(1):23-29. https://doi.org/10.1016/j.brachy.2015.09.012
35. Iftimia I, Cirino ET, Mower HW, McKee AB. Treatment planning methodology for the Miami Multichannel

Applicator following the American Brachytherapy Society recently published guidelines: the Lahey Clinic experience. Journal of Applied Clinical Medical Physics. 2013 01;14(1):214-227. https://doi.org/10.1120/jacmp.v14i1.4098
36. Biltekin F, Akyol H, Gültekin M, Yildiz F. 3D printer-based novel intensity-modulated vaginal brachytherapy applicator: feasibility study. Journal of Contemporary Brachytherapy. 2020;12(1):17-26. https://doi.org/10.5114/jcb.2020.92407
37. Krishnamurthy R, Gurram L, Ghadi Y, Aravindhan D, Scaria L, Kohle S, Kadam S, Chopra S, Mahantshetty U. Modified Houdek vault applicator for high-dose-rate brachytherapy: a technical report and case series. Journal of Contemporary Brachytherapy. 2021;13(6):649-654. https://doi.org/10.5114/jcb.2021.112116
38. Kim SW, Jeong C, Chang KH, Ji YS, Cho B, Lee D, Kim YS, Song SY, Lee SW, Kwak J. Development of 3D Printed Applicator in Brachytherapy for Gynecologic Cancer. International Journal of Radiation Oncology, Biology, Physics. 2017 Oct 01;99(2):E678. https://doi.org/10.1016/j.ijrobp.2017.06.2238
39. Zhao Z, Tang X, Mao Z, Zhao H. The design of an individualized cylindrical vaginal applicator with oblique guide holes using 3D modeling and printing technologies. Journal of Contemporary Brachytherapy. 2019;11(5):479-487. https://doi.org/10.5114/jcb.2019.88441
40. Cameron AL, Cornes P, Al-Booz H. Brachytherapy in endometrial cancer: Quantification of air gaps around a vaginal cylinder. Brachytherapy. 2008 Oct;7(4):355-358. https://doi.org/10.1016/j.brachy.2008.07.004